Supporting Information

Designing dynamic coordination bonds in polar hybrid crystals for high-temperature ferroelastic transition

Yao-Bin Li,[a] Xiao-Xian Chen,[a] Wei-Jian Xu,[b] Ya-Ping Gong,[a] Hui Ye,[a] Zhi-Shuo Wang,[a] and Wei-Xiong Zhang*[,a]

[a] MOE Key Laboratory of Bioinorganic and Synthetic Chemistry, School of Chemistry, IGCME, Sun Yat-Sen University, Guangzhou 510275, China.

[b] Department of Chemistry & CICECO-Aveiro Institute of Materials, University of Aveiro, 3810-193 Aveiro, Portugal

E-mail: zhangwx6@mail.sysu.edu.cn

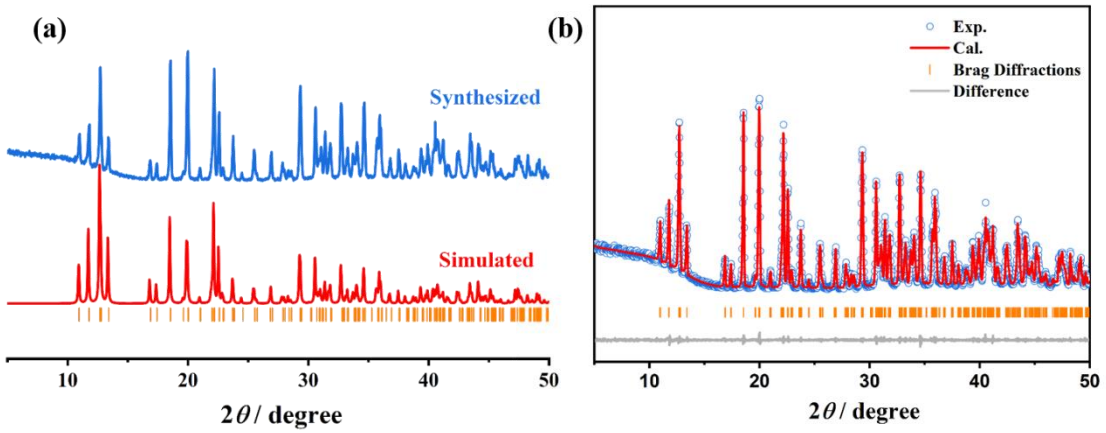

Fig S1. (a) The PXRD patterns of simulated and synthesized samples for **1.** (b) Pawley refinement on the PXRD pattern of **1** at 295 K reveals the presence of a monoclinic unit cell: a = 8.967(2) Å, b = 8.934(2) Å, c = 13.891(2) Å, γ = 115.129(1)º, V =1007.50(2) Å^3 (residuals R_{wp} = 5.03%, R_p = 3.93%), in space group $P112_1$. Experimental pattern (blue circles), calculated pattern (red line), brag diffractions (orange line) and difference profile (grey line). The difference profile reveal well agreements between the experimental PXRD pattern and the simulated one.

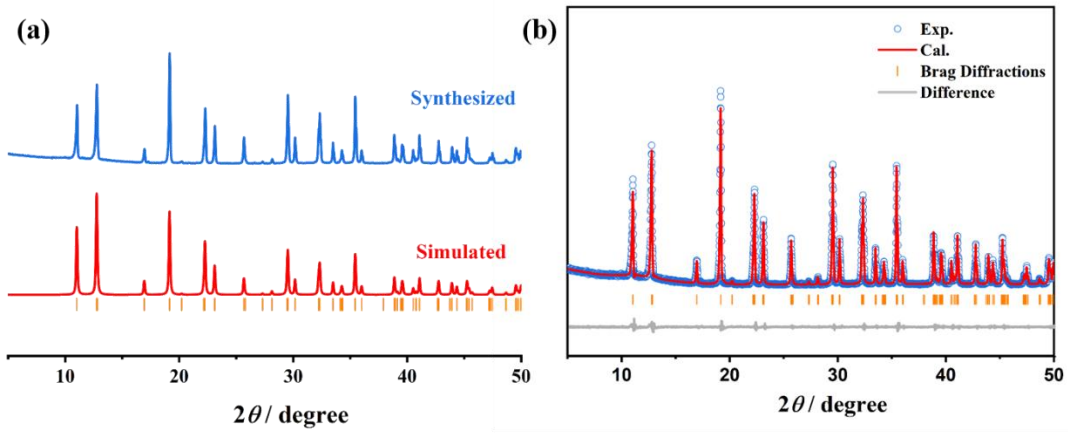

Fig S2. (a) The PXRD patterns of simulated and synthesized samples for **2**. (b) Pawley refinement on the PXRD pattern of **2** at 295 K reveals the presence of a hexagonal unit cell: a = 9.269(1) Å, b = 9.269(1) Å, c = 13.803(1) Å, V =1026.99(2) Å^3 (residuals R_{wp} = 5.80%, R_p = 4.40%), in space group $P6_3$. Experimental pattern (blue circles), calculated pattern (red line), brag diffractions (orange line) and difference profile (grey line)**.** The difference profile reveal well agreements between the experimental PXRD pattern and the simulated one.

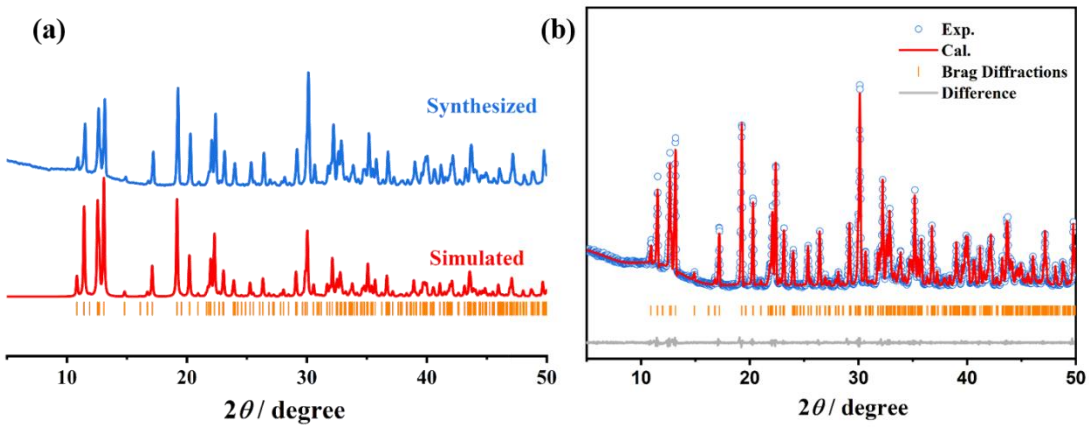

Fig S3. (a) The PXRD patterns of simulated and synthesized samples for **3**. (b) Pawley refinement on the PXRD pattern of **3** at 295 K reveals the presence of an orthorhombic unit cell: a = 16.331(1) Å, b = 8.786(1) Å, c = 13.951(1) Å, V = 2001.75(2) Å^3 (residuals R_{wp} = 5.18%, R_p = 3.83%), in space group $Pna2_1$. Experimental pattern (blue circles), calculated pattern (red line), brag diffractions (orange line) and difference profile (grey line)**.** The difference profile reveal well agreements between the experimental PXRD pattern and the simulated one.

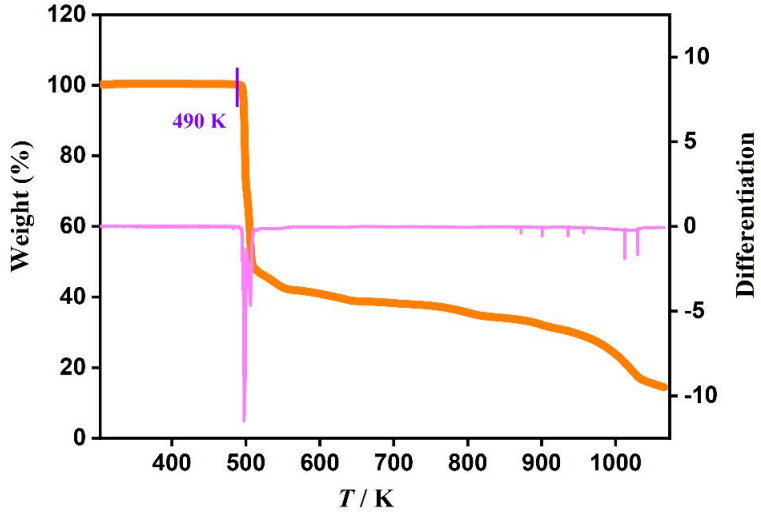

Fig S4. Thermogravimetry curve and differentiation curve of **1**.

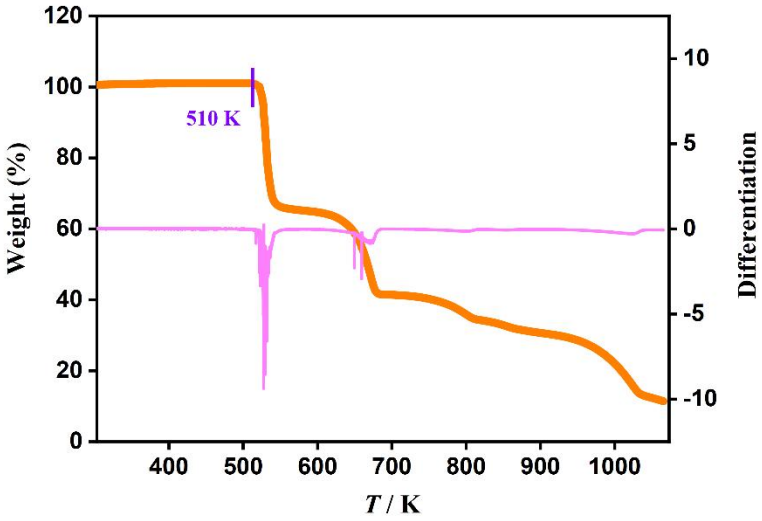

Fig S5. Thermogravimetry curve and differentiation of **2**.

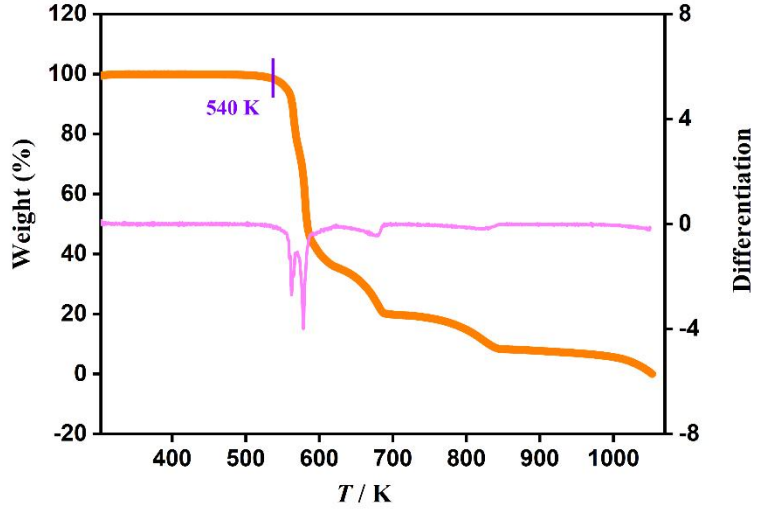

Fig S6. Thermogravimetry curve and differentiation of **3**.

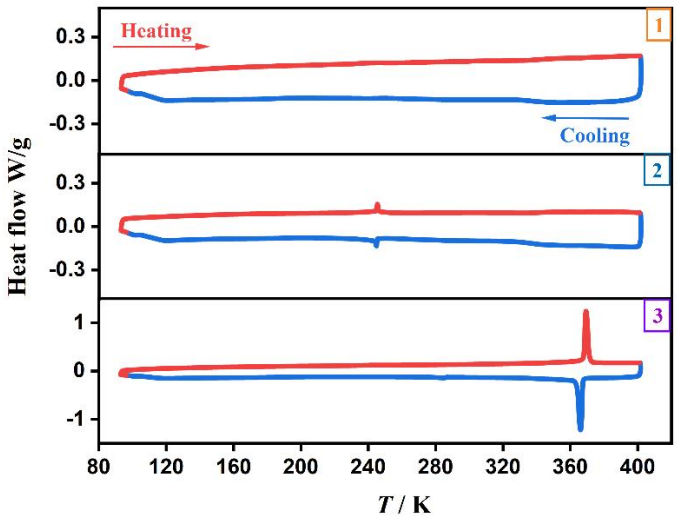

Fig S7. DSC curves in temperature range of 90-400 K for **1**, **2**, and **3**.

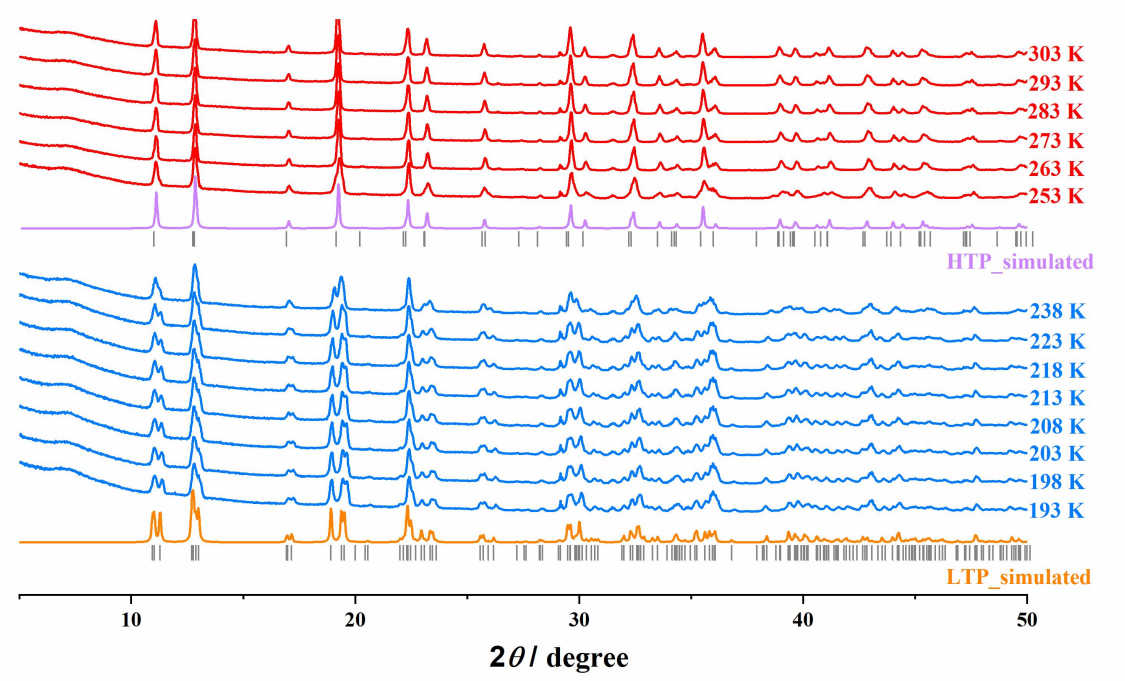

Fig. S8. The variable-temperature experimental PXRD patterns of **2**.

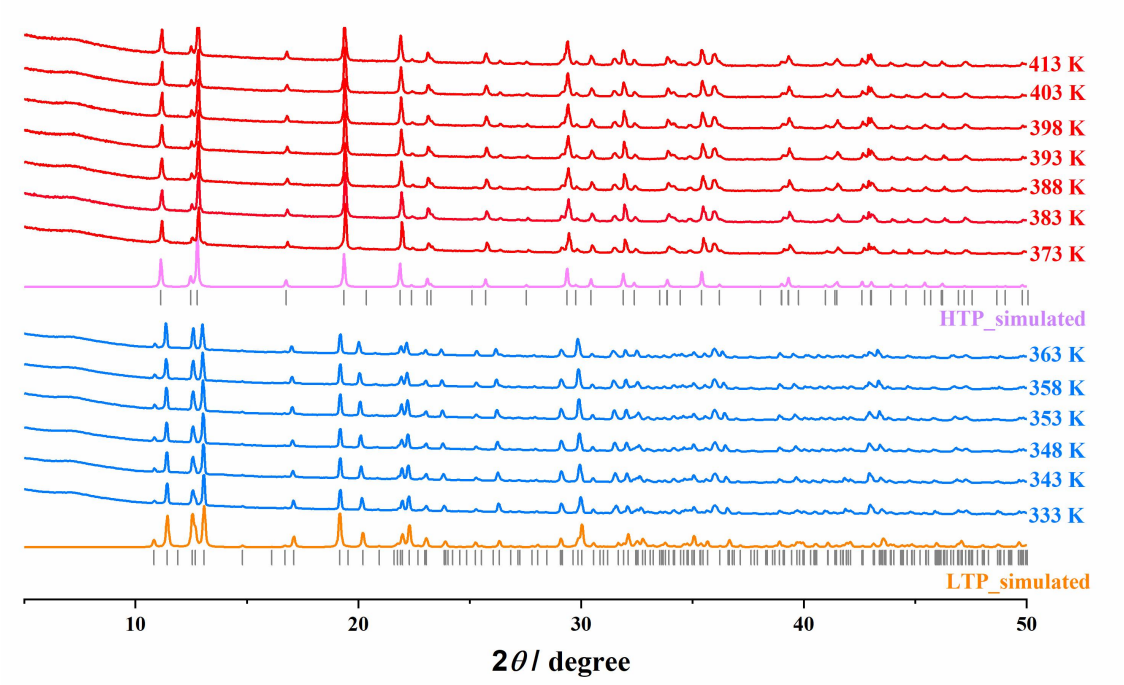

Fig. S9. The variable-temperature experimental PXRD patterns of **3**.

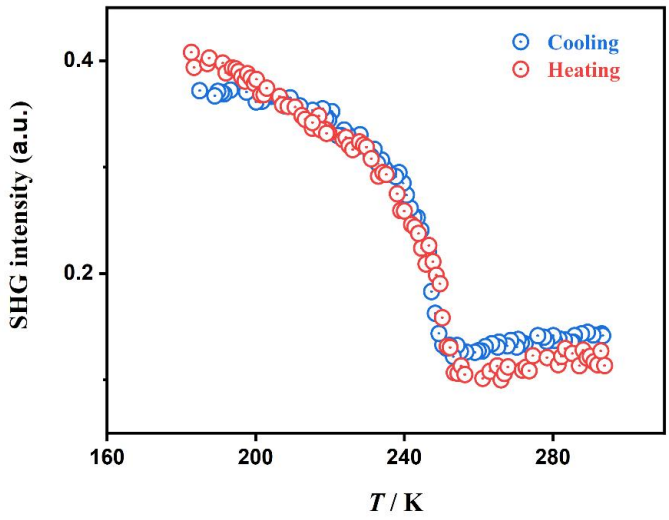

Fig S10. The temperature-dependent SHG signal in the heating and cooling cycle for **2**.

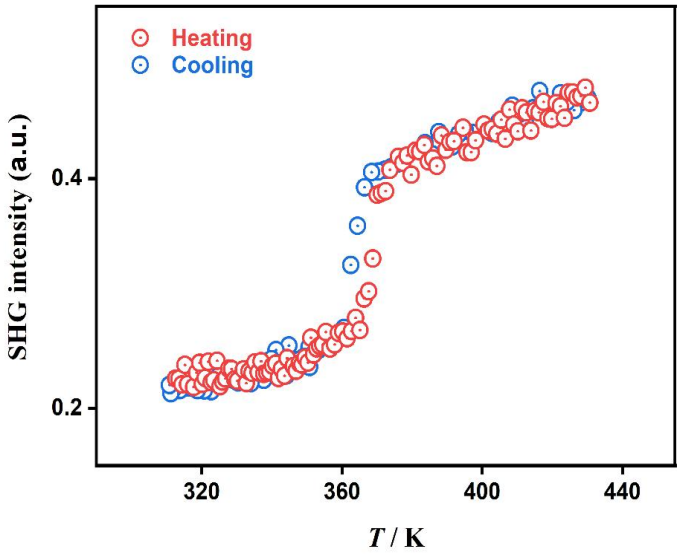

Fig S11. The temperature-dependent SHG signal in the heating and cooling cycle for **3**.

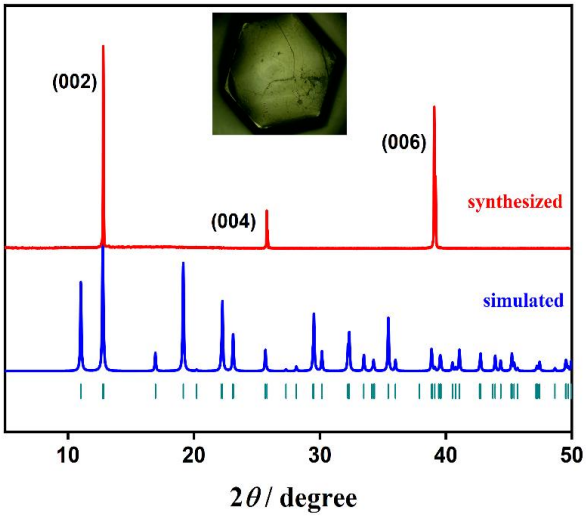

Fig S12. The PXRD patterns measured on the largest plane of single crystal of **2** for observation of ferroelastic domains.

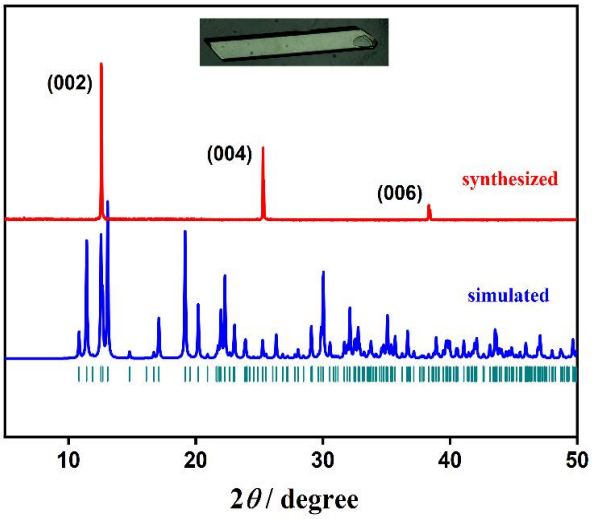

Fig S13. The PXRD patterns measured on the largest plane of single crystal of **3** for observation of ferroelastic domains

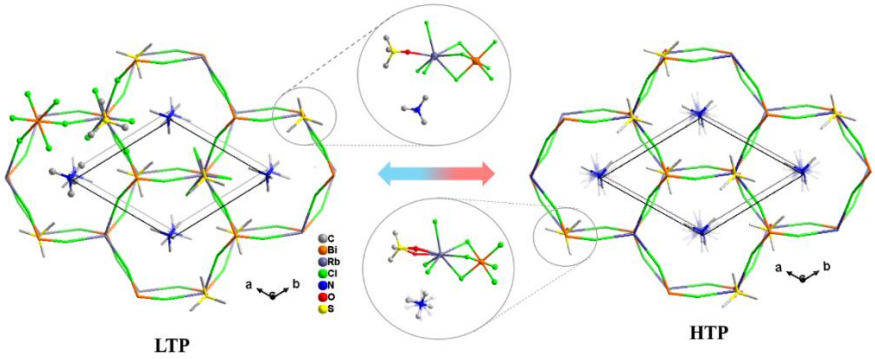

Fig. S14. Crystal packing structures along the *c* axis in **2_LTP** and **2_HTP**. For clarity, all H atoms are omitted.

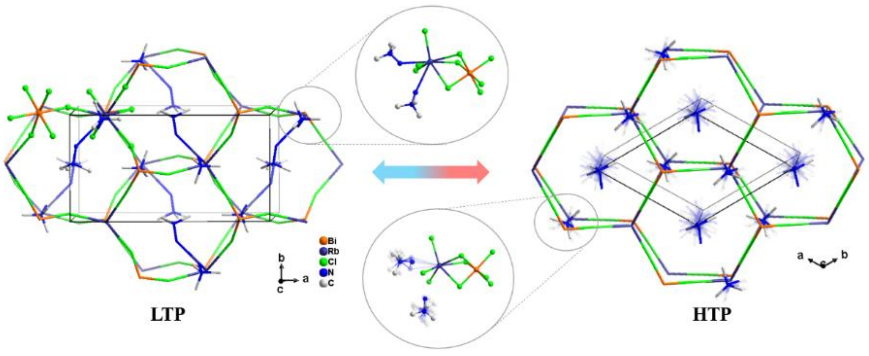

Fig. S15. Crystal packing structures along the *c*-axis in **3_LTP** and **3_HTP**. For clarity, all H atoms are omitted.

Table S1 Crystal data and structural refinement parameters for **1** and **2.**

Compound	$(Me_3SO)_2[RbBiCl_6]$ (**1**)	$(Me_3SO)(Me_4N)[RbBiCl_6]$ (**2**)	
Formula weight	693.47	674.46	
Phase	/	**2_LTP**	**2_HTP**
Temperature (K)	210(2)	205(9)	275(3)
Crystal system	monoclinic	monoclinic	hexagonal
Space group	$P112_1$	$P112_1$	$P6_3$
a / Å	8.8896(4)	9.0947(10)	9.2604(5)
b / Å	8.9063(3)	9.1571(11)	9.2604(5)
c / Å	13.8233(4)	13.7302(8)	13.8004(7)
γ / º	115.000(5)	118.189(15)	120
V / Å^3	991.90(7)	1007.8(2)	1024.91(12)
Z	2	2	2
D_c / (g cm^{-3})	2.322	2.222	2.185
R_1 [$I > 2\sigma(I)$][a]	0.0250	0.0590	0.0358
wR_2 [$I > 2\sigma(I)$][b]	0.0481	0.1516	0.0880
GOF	1.038	1.050	1.062
CCDC number	2313518	2313517	2313516

Table S2 Crystal data and structural refinement parameters for **3.**

Compound	$(Me_3NNH_2)_2[RbBiCl_6]$ (**3**)	
Formula weight	657.42	
Phase	**3_LTP**	**3_HTP**
Temperature (K)	304(6)	393(5)
Crystal system	orthorhombic	hexagonal
Space group	$Pna2_1$	$P6_3mc$
a / Å	16.3250(7)	9.1623(8)
b / Å	8.7816(4)	9.1623(8)
c / Å	13.9451(5)	14.1774(10)
γ/ º	90	120
V / Å^3	1999.16(14)	1030.71(19)
Z	4	2
D_c / (g cm^{-3})	2.184	2.118
R_1 [$I > 2\sigma(I)$][a]	0.0399	0.0476
wR_2 [$I > 2\sigma(I)$][b]	0.0770	0.1031
GOF	1.026	1.043
CCDC number	2313519	2313598

[a] $R_1 = \sum||F_o| - |F_c||/\sum|F_o|$, [b] $wR_2 = \{\sum w[(F_o)^2 - (F_c)^2]^2/\sum w[(F_o)^2]^2\}^{1/2}$

[c] $R_p = \Sigma|cY_{sim}(2\theta_i) - I^{exp}(2\theta_i) + Y^{back}(2\theta_i)|/\Sigma|I^{exp}(2\theta_i)|$.

[d] $R_{wp} = \{w_p[cY_{sim}(2\theta_i) - I^{exp}(2\theta_i) + Y^{back}(2\theta_i)]^2/\Sigma w_p[I^{exp}(2\theta_i)]^2\}^{1/2}$, and $w_p = 1/I^{exp}(2\theta_i)$.

Table S3. Bond Lengths for **1.**

Atom	Atom	Length/Å	Atom	Atom	Length/Å
Bi1	Cl1	2.7192(14)	Rb1	Cl6[3]	3.4483(18)
Bi1	Cl2	2.7885(16)	Rb1	O1	2.782(7)
Bi1	Cl3	2.6822(15)	Rb1	O2	2.995(6)
Bi1	Cl4	2.6977(14)	S1	O1	1.432(7)
Bi1	Cl5	2.6490(16)	S1	C1	1.733(6)
Bi1	Cl6	2.7286(17)	S1	C2	1.714(7)
Rb1	Cl1	3.3885(15)	S1	C3	1.704(8)
Rb1	Cl2	3.4444(19)	S2	O2	1.422(6)
Rb1	Cl3	3.4081(18)	S2	C4	1.729(9)
Rb1	Cl4[1]	3.3461(16)	S2	C5	1.688(10)
Rb1	Cl5[2]	3.3630(18)	S2	C6	1.712(7)

[1]1-X, 1-Y, 1/2+Z; [2]-X, -Y, 1/2+Z; [3]1-X, -Y, 1/2+Z.

Table S4. Bond Lengths for **2** at LTP**.**

Atom	Atom	Length/Å	Atom	Atom	Length/Å
Bi1	Cl1	2.697(6)	Rb1	Cl6	3.321(7)
Bi1	Cl2	2.703(6)	Rb1	O1	2.74(4)
Bi1	Cl3	2.714(6)	S1	O1	1.42(4)
Bi1	Cl4	2.733(7)	S1	C1	1.73(3)
Bi1	Cl5	2.668(6)	S1	C2	1.73(2)
Bi1	Cl6	2.745(6)	S1	C3	1.71(3)
Rb1	Cl1[1]	3.334(7)	N1	C4	1.487(18)
Rb1	Cl2[2]	3.404(7)	N1	C5	1.484(18)
Rb1	Cl3	3.324(7)	N1	C6	1.478(18)
Rb1	Cl4	3.309(7)	N1	C7	1.474(18)
Rb1	Cl5[3]	3.415(7)			

[1]1-X, 1-Y, -1/2+Z; [2]1-X,-Y, -1/2+Z; [3]2-X, 1-Y, -1/2+Z.

Table S5. Bond Lengths for **3** at LTP.

Atom	Atom	Length/Å	Atom	Atom	Length/Å
Bi1	Cl1	2.685(3)	Rb1	Cl6[3]	3.217(3)
Bi1	Cl2	2.736(3)	Rb1	N1	3.119(9)
Bi1	Cl3	2.717(3)	Rb1	N3	3.535(11)
Bi1	Cl4	2.716(3)	N1	N2	1.435(13)
Bi1	Cl5	2.710(3)	N2	C1	1.479(15)
Bi1	Cl6	2.710(3)	N2	C2	1.472(16)
Rb1	Cl1	3.570(4)	N2	C3	1.470(14)
Rb1	Cl2	3.277(3)	N3	N4	1.446(14)
Rb1	Cl3[1]	3.401(3)	N4	C4	1.469(14)
Rb1	Cl4[2]	3.387(3)	N4	C5	1.501(17)
Rb1	Cl5	3.420(3)	N4	C6	1.464(19)

[1]1/2-X, -1/2+Y, 1/2+Z; [2]1-X, 2-Y, 1/2+Z; [3]1/2-X, 1/2+Y, 1/2+Z.

Table S6. Pawley refinements results on the variable-temperature powder X-ray diffraction patterns of **2**.

Phase	Temperature / K	*a* / Å	*b* / Å	*c* / Å	*V* / Å^3	R_p / %	R_{wp} / %
LTP	193	9.067(1)	9.159(1)	13.704(2)	1004.66	2.80	4.46
	198	9.075(1)	9.163(1)	13.710(2)	1005.91	2.78	4.49
	203	9.082(1)	9.167(1)	13.715(2)	1006.91	2.85	4.50
	208	9.091(1)	9.172(1)	13.719(2)	1008.07	2.77	4.51
	213	9.101(1)	9.178(1)	13.727(1)	1009.79	2.80	4.41
	218	9.108(1)	9.182(1)	13.732(1)	1010.59	2.74	4.36
	223	9.118(1)	9.188(1)	13.737(1)	1011.87	2.67	4.27
	238	9.144(6)	9.200(6)	13.753(9)	1013.53	2.81	4.64
HTP	253	9.248(1)	9.248(1)	13.783(1)	1020.87	2.88	4.56
	263	9.253(1)	9.253(1)	13.787(1)	1022.27	2.80	4.35
	273	9.258(1)	9.258(1)	13.792(1)	1023.75	2.76	4.23
	283	9.263(1)	9.263(1)	13.798(1)	1025.30	2.76	4.17
	293	9.267(1)	9.267(1)	13.802(1)	1026.48	2.73	4.00
	303	9.272(1)	9.272(1)	13.808(1)	1028.03	2.72	4.09

Table S7. Pawley refinements results on the variable-temperature powder X-ray diffraction patterns of **3**.

Phase	Temperature / K	a / Å	b / Å	c / Å	V / Å^3	R_p / %	R_{wp} / %
LTP	333	16.321(1)	8.817(1)	13.985(1)	2012.47(1)	2.80	4.29
	343	16.309(1)	8.831(1)	14.001(1)	2016.49(1)	2.55	3.90
	348	16.303(1)	8.839(1)	14.010(1)	2018.87(1)	2.65	3.94
	353	16.294(1)	8.849(1)	14.021(1)	2021.63(1)	2.61	3.89
	358	16.285(1)	8.860(1)	14.029(1)	2024.18(1)	2.60	3.82
	363	16.273(1)	8.875(1)	14.044(1)	2028.28(1)	2.49	3.68
		*$3^{1/2}$					
HTP	373	15.864(1)	9.159(1)	14.145(1)	2055.25(1)	2.81	4.10
	383	15.872(1)	9.164(1)	14.158(1)	2059.29(1)	2.52	3.66
	388	15.875(1)	9.165(1)	14.166(1)	2061.07(1)	2.52	3.65
	393	15.877(1)	9.167(1)	14.172(1)	2062.66(1)	2.47	3.66
	398	15.881(1)	9.169(1)	14.178(1)	2064.50(1)	2.55	3.70
	403	15.885(1)	9.171(1)	14.188(1)	2066.93(1)	2.55	3.76
	413	15.891(1)	9.175(1)	14.201(1)	2070.51(1)	2.66	3.96

Table S8. Liner fitting results of variable-temperature cell parameters of **2**.

Phase	Fitting equations	R^2	Deduced parameters at T_1 (245K)
LTP	$a = 0.00172T + 8.73347$	0.999	9.155 Å
	$b = 0.000938655T + 8.97736$	0.997	9.207 Å
	$c = 0.00109T + 13.49312$	0.998	13.760 Å
	$\beta = 0.01406T + 115.29098$	0.997	118.878°
			V = 1015.61 Å^3
HTP	$a = 0.000477143T + 9.12752$	0.999	9.244 Å
	$b = 0.000477143T + 9.12752$	0.999	9.244 Å
	$c = 0.000502857T + 13.65521$	0.997	13.778 Å
			V = 1019.62 Å^3

Table S9. Liner fitting results of variable-temperature cell parameters of **3**.

Phase	Fitting equations	R^2	Deduced parameters at T_1 (369 K)
LTP	a = -0.00158T + 16.84897	0.978	16.267 Å
	b = 0.00192T + 8.17544	0.980	8.884 Å
	c = 0.00192T +13.34224	0.992	14.051 Å
			V = 2030.59 Å^3
HTP	a = 0.00066098T +15.61811	0.998	15.862 Å
	b = 0.000370667T +9.02142	0.989	9.158 Å
	c = 0.00142T+13.61464	0.998	14.139 Å
			V = 2053.89 Å^3

Table S10. Thermal expansion coefficients of the principal axes in **2** and **3**.

Phase	T/K	Principl eaxis	Directions a	b	c	α/MK^{-1}	β_V/MK^{-1}
2_LTP	193-238	X_1	0.6297	0.7768	0.0000	-68(2)	
		X_2	0.0000	0.0000	1.0000	79(1)	240(1)
		X_3	-0.8841	0.4674	0.0000	228(2)	
2_HTP	253-303	X_1	0.0000	0.0000	1.0000	36(1)	
		X_2	0.0000	1.0000	0.0000	51(1)	140(1)
		X_3	-0.8944	-0.4473	0.0000	51(1)	
3_LTP	333-363	X_1	-1.0000	0.0000	0.0000	96(7)	
		X_2	0.0000	0.0000	1.0000	140(7)	260(17)
		X_3	0.0000	-1.0000	0.0000	215(16)	
3_HTP	373-413	X_1	1.0000	0.0000	0.0000	42(1)	
		X_2	0.0000	1.0000	0.0000	42(1)	185(1)
		X_3	0.0000	0.0000	1.0000	99(1)	

The calculation of the spontaneous strain

For the present 6*F*2 species of **2,** the spontaneous strain tensor is given as:

$$\varepsilon_{ij} = \begin{bmatrix} \frac{asin\gamma}{a_0 sin\gamma_0} - 1 & \frac{1}{2}\left(\frac{acos\gamma}{a_0 sin\gamma_0} - \frac{bcos\gamma_0}{b_0 sin\gamma_0}\right) & 0 \\ \frac{1}{2}\left(\frac{acos\gamma}{a_0 sin\gamma_0} - \frac{bcos\gamma_0}{b_0 sin\gamma_0}\right) & \frac{b}{b_0} - 1 & 0 \\ 0 & 0 & \frac{c}{c_0} - 1 \end{bmatrix} \text{ (equation 1)}$$

In the equation, a, b, c, and γ refer to the low-symmetry form of **2 (**at LTP), and a_0, b_0, c_0, and γ_0 are the cell parameters of high-symmetry form **(**at HTP). The cell parameters are from deduced results in Table S8.

For the present 6*mmFmm*2 species of **3,** the spontaneous strain tensor is given as:

$$\varepsilon_{ij} = \begin{bmatrix} \frac{a}{a_0} - 1 & 0 & 0 \\ 0 & \frac{b}{b_0} - 1 & 0 \\ 0 & 0 & \frac{c}{c_0} - 1 \end{bmatrix} \text{ (equation 2)}$$

In the equation, a, b, c refer to the low-symmetry form of **3 (**at LTP), and a_0, b_0, c_0, and γ_0 are the converted orthorhombic cell parameters of high-symmetry form **(**at HTP). The cell parameters are from deduced results in Table S9.

The total spontaneous strain ε_{ss} can be given as: [S1-S3]

$$\varepsilon_{ss} = \sqrt{\sum_{ij} \varepsilon_{ij}^2} \; (i = 1,2,3; j = 1,2,3) \text{ (equation 3)}$$

References

S1. K. Aizu, *J. Phys. Soc. Jpn.*, 1970, **28**, 706-716.

S2. J. Sapriel, *Phys. Rev. B*, 1975, **12**, 5128-5140

S3. M. A. Carpenter, E. K. H. Salje and A. Graeme-Barber, *Eur. J. Mineral.*, 1998, **10**, 621-691.